

# In-Situ Formation of ZnO Nanobelts and Metallic Zn Nanobelts and Nanodisks

Yanfa Yan,<sup>\*,†</sup> Ping Liu,<sup>†</sup> J. G. Wen,<sup>‡</sup> B. To,<sup>†</sup> and M. M. Al-Jassim<sup>†</sup>

National Renewable Energy Laboratory, Golden, Colorado 80401, and Frederick Seitz Materials Research Laboratory, University of Illinois at Urbana-Champaign, Urbana, Illinois 61801

Received: March 11, 2003; In Final Form: May 19, 2003

We report on the in-situ formation of ZnO nanobelts and metallic Zn nanobelts and nanodisks in a transmission electron microscope by electron-beam irradiation of single-crystalline polyhedral Zn nanoparticles, which were synthesized by evaporating ZnO powder mixed with graphite in a N<sub>2</sub> flowing carrying gas environment. ZnO and Zn nanobelts are both single-crystalline, have a top surface of  $\pm\{110\}$ , a side surface of  $\pm\{100\}$ , and a  $\pm[001]$  growth direction. The zinc nanodisks have diameters of 10 nm to 0.3  $\mu\text{m}$ , and thickness of about 0.1  $\mu\text{m}$ . They usually have faceted hexagonal shapes with a top surface of  $\pm(001)$ .

## Introduction

Because of their novel electronic properties, low-dimensional nanostructures are considered the building blocks for future nanoscale electronic and optoelectronic nanodevices.<sup>1–3</sup> In the past decade, the development of new techniques to synthesize nanomaterials has attracted great attention. Many methods were developed for synthesizing nanostructures with different morphologies such as nanorods, nanowires, nanoparticles, and quantum dots. To date, a wide range of materials, including metals,<sup>4–9</sup> semiconductors,<sup>10–13</sup> and metal oxides<sup>14–19</sup> have been made into nanostructures. Of these, metallic nanostructures have shown enhanced physical, optical, and electronic properties.<sup>4</sup> In addition, metallic nanowires are potential candidates for nanoconnectors in nanoscale devices. Thus, extensive efforts have been made to synthesize metallic nanostructures. A variety of methods have been developed to synthesize various-shaped metallic nanoparticles, nanorods, nanodisks, nanoparticles, and nanowires. Successful methods include colloidal synthesis, template synthesis, step-edge decoration, and photon-induced synthesis.<sup>4–9</sup> Recently, an interesting phenomenon was reported by Pan et al.<sup>20</sup> They found that Pb nanocrystals with a spherical shape can be produced by irradiating larger polyhedral Pb particles. Their results indicate that nanocrystals of metals with low melting points could be produced in-situ in a transmission electron microscope (TEM) by electron-beam irradiation.

Here, we demonstrate that ZnO nanobelts and metallic Zn nanobelts and nanodisks can be formed in-situ in a TEM by electron-beam irradiation of single-crystalline Zn nanoparticles. The Zn nanoparticles, with diameters of 1 to 6  $\mu\text{m}$ , were synthesized by evaporating ZnO powder mixed with graphite in a N<sub>2</sub> flowing carrying gas environment. TEM and energy-dispersive X-ray spectroscopy (EDS) analyses revealed that electron-beam irradiation-induced ZnO nanobelts and metallic Zn nanobelts and nanodisks are single-crystalline and free from structural defects. The ZnO and Zn nanobelts both have a top surface of  $\pm\{110\}$ , a side surface of  $\pm\{100\}$ , and the growth direction of  $\pm[001]$ . The Zn nanodisks have faceted shapes of

hexagonal projection. The top surfaces of the Zn nanodisks are  $\pm(001)$ . The diameters of the nanodisks range from 10 nm to 0.3  $\mu\text{m}$ .

## Experimental Section

The synthesis of polyhedral Zn nanoparticles was carried out in a quartz tube, with N<sub>2</sub> used as a carrying gas. The source material, which is pure ZnO powder mixed with graphite (molar ratio of 1:1), was placed in a quartz crucible that was then placed in the middle of the quartz tube. The N<sub>2</sub> flowing rate was about 50 sccm (standard cubic centimeters per minute). The quartz tube was inserted into a horizontal tube furnace, which was heated at a rate of 20–30 °C/min to 1100 °C. A quartz plate was placed in the downstream end of the quartz tube. Its temperature, monitored by a thermocouple diode, was about 200–300 °C during growth. After a 30-min evaporation, the quartz tube was taken out of the furnace and cooled to room temperature. N<sub>2</sub> gas was kept flowing during the cooling. Fluffy dark-gray products formed on both the quartz plate and nearby areas on the inner wall of the quartz tube. The morphology of the as-deposited products was analyzed by a scanning electron microscope (SEM) (JEOL JSM6320F). Electron-beam irradiation of Zn polyhedrons was performed in a TEM (Philips CM30) operated at 300 kV. The structure and chemical compositions of the electron-beam irradiation-induced Zn nanobelts and nanodisks were analyzed by electron diffraction and EDS.

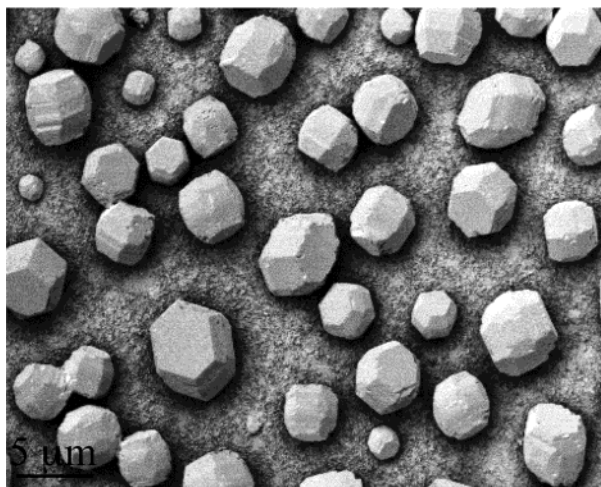
## Results and Discussion

Figure 1 shows a SEM image of the as-deposited products synthesized by evaporating ZnO powder mixed with graphite in a N<sub>2</sub> flowing carrying gas environment. It reveals that the as-deposited products consist of a large quantity of nanoparticles with faceted geometrical shapes. The diameters of these polyhedrons are in the range of 1 to 6  $\mu\text{m}$ . X-ray diffraction analyses showed that the as-deposited products are crystalline Zn metals. EDS spectra obtained from the edge of the polyhedrons in TEM confirmed that the composition is Zn. Electron diffraction taken from different positions around the edge of the polyhedrons showed consistent patterns, verifying that the polyhedral Zn nanoparticles are single crystals.

\* Corresponding author. E-mail: yyan@nrel.gov.

<sup>†</sup> National Renewable Energy Laboratory.

<sup>‡</sup> Frederick Seitz Materials Research Laboratory, University of Illinois at Urbana-Champaign.



**Figure 1.** SEM image of as-synthesized polyhedral Zn nanoparticles.

The presence of carrying gas is important in forming for the polyhedral Zn nanoparticles in our synthesis. At a high-temperature condition (1100 °C), carbon reacts with ZnO to form Zn vapor and CO<sub>2</sub>. Because of the presence of N<sub>2</sub>-carrying gas, oxygen concentration should be very low in the quartz tube. Thus, only a small portion of the Zn vapor will be converted to ZnO, which will start to condense into ZnO crystals at about 800 °C. Because Zn has a much lower melting temperature (about 419 °C) than ZnO (about 1975 °C), the majority of the vapor being carried to the low-temperature zone would be Zn. At low temperatures, such as 200–300 °C, Zn vapor could condense to form Zn nanoparticles.

Figure 2a is a bright-field TEM image showing a Zn nanoparticle with a diameter of about 5 μm. It is seen that the area surrounding the Zn particle is clean, without any smaller objects. We found that when a strong electron beam was focused on the Zn particle, the particle melted quickly. The Zn particle broke down and formed small Zn droplets. A fraction of the Zn particle erupted off, and metallic Zn nanobelts and nanodisks formed instantly in the nearby areas on the carbon supporting film. The Zn droplets moved around under the electron beam and then changed into ZnO nanobelts and nanosheets. The residual air in the TEM chamber was the possible oxygen source. The vacuum in the TEM chamber was about 10<sup>-7</sup> Torr. The process took place in a short period of time, usually within a second. Figure 2b shows the corresponding results after the Zn particle was irradiated by a strong convergent electron beam. It is seen that the polyhedral Zn particle transformed into two parts: a dense residual-like portion and scattered nanobelts and nanodisks (the lower part in Figure 2b). The arrows, marked by 1, 2, and 3, in Figures 2a and 2b indicate the corresponding features of the supporting carbon film, revealing that Figures 2a and 2b were taken from the same area. It is thus evident that the nanostructures shown in Figure 2b were formed in-situ by electron-beam irradiation of the Zn nanoparticles shown in Figure 2a.

TEM and EDS analyses revealed that the dense residual-like portion is comprised of ZnO nanobelts and thin sheets. Figure 3a shows a bright-field TEM image of an area in this portion, clearly revealing the morphology of nanobelts. The ZnO nanobelts are found to orient randomly. Figure 3b shows an EDS spectrum taken from a nanobelt, verifying the presence of O and Zn. Electron diffraction patterns taken from the nanobelts confirmed that the nanobelts are ZnO. Consistent electron diffraction patterns obtained through the entire length of the nanobelts indicated that the ZnO nanobelts are single

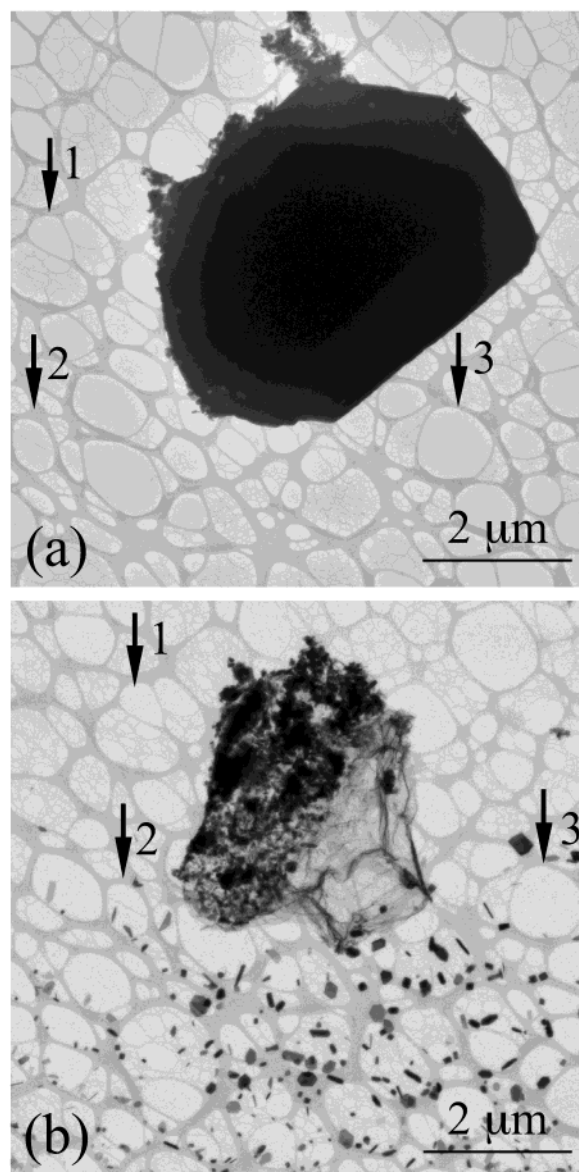


**Figure 2.** Bright-field TEM image of polyhedral Zn nanoparticle (a) before strong electron-beam irradiation, (b) after irradiation by a convergent electron beam.

crystals. Electron diffraction analysis indicated that the ZnO nanobelts have top surfaces of  $\pm\{110\}$  and side surfaces of  $\pm\{100\}$ . Their growth direction is  $\pm[001]$ . The inset in Figure 3a is an electron diffraction pattern along a  $\langle 110 \rangle$  zone axis taken from a ZnO nanobelt. The thickness of the nanobelts is estimated to be less than 50 nm. Because the growth occurred within a second, the ZnO nanobelts are usually very short, with lengths usually less than 200 nm.

Figures 4a and 4b are bright-field TEM images showing the metallic Zn nanobelts and nanodisks, respectively, formed in-situ by electron-beam irradiation. EDS analyses revealed that both the nanobelts and nanodisks are pure Zn. Figure 4c shows a typical EDS spectrum taken from the nanobelts and nanodisks, verifying the presence of only Zn, without detectable O. Electron microdiffraction analyses indicate that the Zn nanobelts and nanodisks are single crystals and free from structural defects. The inset in Figure 4a is a convergent beam electron diffraction pattern along a  $\langle 110 \rangle$  zone axis taken from a Zn nanobelt. The inset in Figure 4b is a convergent beam electron diffraction patterns along a  $\langle 001 \rangle$  zone axis taken from a Zn nanodisk.

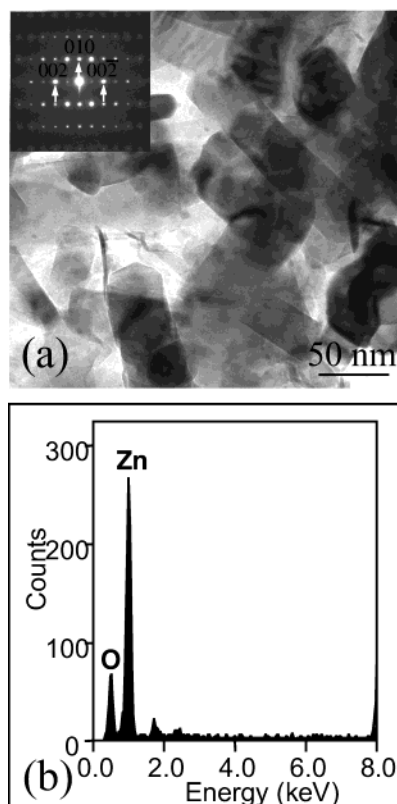


**Figure 3.** (a) Bright-field TEM image of ZnO nanobelts formed by irradiating the Zn particle shown in Figure 2a with a convergent electron beam; (b) typical EDS spectrum taken from ZnO nanobelts, verifying the presence of O and Zn.

Diffraction analyses reveal that the zinc nanobelts have a top surface of  $\pm\{110\}$  and a side surface of  $\pm\{100\}$  and their growth direction is  $\pm[001]$ . The diameters of Zn nanodisks range from 10 nm to  $0.3\ \mu\text{m}$ . The thickness of the nanodisks is estimated to be less than  $0.1\ \mu\text{m}$ . Most of the Zn nanodisks have the faceted geometrical shape of a hexagonal projection. Their top surfaces are  $\pm(001)$  crystal planes, and their side surfaces are  $\pm\{110\}$  and  $\pm\{100\}$  crystal planes. These planes are those with lower surface energies in a crystal with hexagonal structure, such as Zn. Some Zn nanodisks show rectangular shapes, as marked by arrows in Figure 4b. This is because they sit on the carbon support film with edge-on due to their very fine sizes.

The mechanism of the electron-beam irradiation-induced formation of ZnO nanobelts and metallic Zn nanobelts and nanodisks in TEM should be similar to that of the formation of nanostructures by thermal evaporation.<sup>19</sup> When a strong electron beam is focused on a Zn particle, the particle melts because of the low melting point of Zn. A portion of the melting Zn will react with oxygen in the TEM to form crystalline ZnO nanobelts at the area where the temperature is proper (above  $600\ ^\circ\text{C}$ ). Simultaneously, some of the melting Zn erupts off and produces Zn vapor. The Zn vapors condense on the low-temperature carbon support film to form Zn nanobelts and nanodisks. Because the temperature of the carbon support film is low, the Zn nanodisks usually have small dimensions.

## Conclusions

We have synthesized metallic polyhedral Zn nanoparticles by evaporating ZnO powder mixed with graphite in a  $\text{N}_2$  flowing carrying gas environment. We found that single-crystalline ZnO

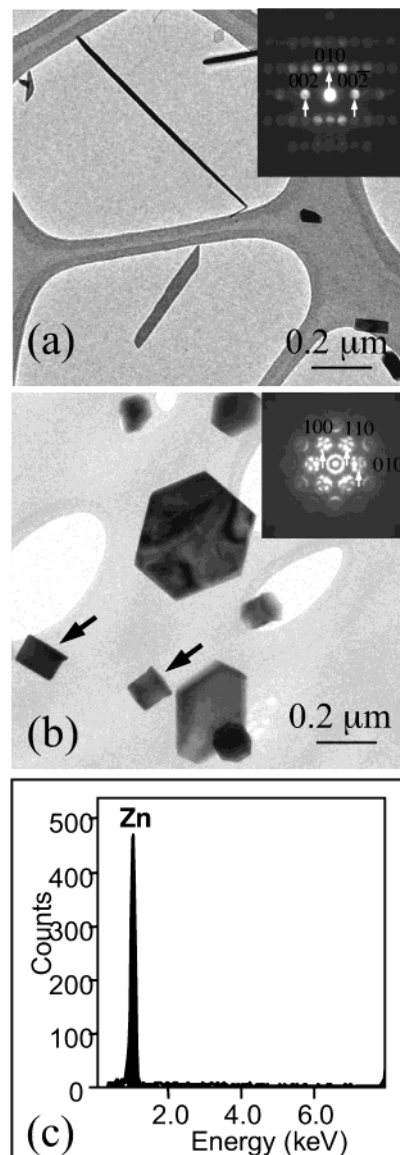


**Figure 4.** Bright-field TEM image of (a) Zn nanobelts and (b) Zn nanodisks formed by irradiating the Zn particle shown in Figure 2a with a convergent electron beam; (c) typical EDS spectrum taken from the Zn nanobelts and nanodisks, verifying the presence of Zn.

nanobelts and metallic Zn nanobelts and nanodisks can be produced in-situ in a TEM by irradiating Zn nanoparticles with a strong convergent electron beam. Both the ZnO and Zn nanobelts have a top surface of  $\pm\{110\}$  and a side surface of  $\pm\{100\}$ , and the growth direction is  $\pm[001]$ . The Zn nanodisks have the faceted shape of a hexagonal projection, with a top surface of  $\pm(001)$ . Their diameters range from 10 nm to  $0.3\ \mu\text{m}$ .

**Acknowledgment.** This work was supported by the U.S. Department of Energy under Contract No. DE-AC36-99GO10337.

## References and Notes

- (1) Alivisatos, A. P. *Science* **1996**, 271, 933.
- (2) Gulseren, O.; Ercolessi, F.; Tosatti, E. *Phys. Rev. Lett.* **1998**, 80, 3775.
- (3) Iijima, S. *Nature* **1991**, 354, 56.
- (4) Lisiecki, I.; Pileni, M.-P. *J. Am. Chem. Soc.* **1993**, 115, 3887.
- (5) Zach, M. P.; Ng, K. H.; Penner, M. *Science* **2000**, 290, 2120.
- (6) Hong, B. H.; Bae, S. C.; Lee, C.-W.; Jeong, S.; Kim, K. S. *Science* **2001**, 294, 348.

- (7) Puentes, V. F.; Krishnan, K. M.; Alivisatos, A. P. *Science* **2001**, *291*, 2115.
- (8) Jin, R.; Cao, Y.; Mirkin, C. A.; Kelly, K. L.; Schatz, G. C.; Zheng, J. G. *Science* **2001**, *294*, 1901.
- (9) Maillard, M.; Giorgio, S.; Pileni, M.-P. *Adv. Mater.* **2002**, *14*, 1084.
- (10) Morales, A. M.; Lieber, C. M. *Science* **1998**, *279*, 208.
- (11) Yu, D. P.; Bai, Z. G.; Ding, Y.; Hang, Q. L.; Zhang, H. Z.; Wang, J. J.; Zou, Y. H.; Qian, W.; Xiong, G. C.; Zhou, H. T.; Feng, S. Q. *Appl. Phys. Lett.* **1998**, *72*, 3458.
- (12) Zhang, Y. F.; Tang, Y. H.; Wang, N.; Lee, C. S.; Bello, I.; Lee, S. T. *Phys. Rev. B* **2000**, *61*, 4518.
- (13) Bae, S. Y.; Seo, H. W.; Park, J.; Yang, H.; Park, J. C.; Lee, S. Y. *Appl. Phys. Lett.* **2002**, *81*, 126.
- (14) Pan, Z. W.; Dai, Z. R.; Wang, Z. L. *Science* **2001**, *291*, 1947.
- (15) Dai, Z. R.; Pan, Z. W.; Wang, Z. L. *Solid State Commun.* **2001**, *118*, 351.
- (16) Kong, Y. C.; Yu, D. P.; Zhang, B.; Fan, W.; Feng, S. Q. *Appl. Phys. Lett.* **2001**, *78*, 407.
- (17) Dai, Z. R.; Pan, Z. W.; Wang, Z. L. *J. Phys. Chem. B* **2002**, *106*, 902.
- (18) Wang, Z. L.; Pan, Z. W. *Adv. Mater.* **2002**, *14*, 1029.
- (19) Yao, B. D.; Chen, Y. F.; Wang, N. *Appl. Phys. Lett.* **2002**, *81*, 757.
- (20) Pan, Z. W.; Dai, Z. R.; Wang, Z. L. *Appl. Phys. Lett.* **2002**, *80*, 309.